

Article

Improved Dielectrically Modulated Quad Gate Schottky Barrier MOSFET Biosensor

Papanasam Esakki ^{1,*} , Prashanth Kumar ¹, Manikandan Esakki ²  and Adithya Venkatesh ¹¹ School of Electronics Engineering, Vellore Institute of Technology Chennai Campus, Chennai 600 127, India² Centre for Innovation and Product Development (CIPD), Vellore Institute of Technology Chennai Campus, Chennai 600 127, India

* Correspondence: papanasam.e@vit.ac.in

Abstract: A novel Schottky barrier MOSFET with quad gate and with source engineering has been proposed in this work. A high- κ dielectric is used at the source side of the channel, while SiO₂ is used at the drain side of the channel. To improve the carrier mobility, a SiGe pocket region is created at the source side of the channel. Physical and electrical characteristics of the proposed device are compared with conventional double gate Schottky barrier MOSFET. It has been observed that the proposed device exhibits better performance, with a higher I_{ON}/I_{OFF} ratio and lower subthreshold slope. The high- κ dielectric, along with the SiGe pocket region, improves tunneling probability, while aluminum, along with SiO₂ at the drain side, broadens the drain/channel Schottky barrier and reduces the hole tunneling probability, resulting in a reduced OFF-state current. Further, the proposed device is used as a biosensor to detect both the charged and neutral biomolecules. Biosensors are made by creating a nanocavity in the dielectric region near the source end of the channel to capture biomolecules. Biomolecules such as streptavidin, biotin, APTES, cellulose and DNA have unique dielectric constants, which modulates the electrical parameters of the device. Different electrical parameters, viz., the electric field, surface potential and drain current, are analyzed for each biomolecule. It has been observed that drain current increases with the dielectric constant of the biomolecules. Furthermore, the sensitivity and selectivity of the proposed biosensors is better than that of conventional biosensors made using double gate Schottky barrier MOSFETs. Sensitivity is almost twice that of a conventional sensor, while selectivity is six to twelve times higher than a conventional one.



Citation: Esakki, P.; Kumar, P.; Esakki, M.; Venkatesh, A. Improved Dielectrically Modulated Quad Gate Schottky Barrier MOSFET Biosensor.

Micromachines **2023**, *14*, 685.

<https://doi.org/10.3390/mi14030685>

Academic Editor: Goutam Koley

Received: 17 February 2023

Revised: 10 March 2023

Accepted: 14 March 2023

Published: 20 March 2023



Copyright: © 2023 by the authors. Licensee MDPI, Basel, Switzerland. This article is an open access article distributed under the terms and conditions of the Creative Commons Attribution (CC BY) license (<https://creativecommons.org/licenses/by/4.0/>).

Keywords: dielectric modulation; Schottky barrier; quad gate; biosensor; MOSFET

1. Introduction

Accurate measurement of important physiological parameters facilitates the timely discovery of potential diseases that deteriorate the health of a patient. The necessity for a early and precise identification of ailments and other vital examinations of living organisms produced a growing need for economic, highly selective and sensitive biosensors. A biosensor is a device which transforms the biological properties of biomolecules into corresponding electrical characteristics. Factors such as inexpensive fabrication, quick response time, congeniality with modern state-of-the-art systems, smaller size and label-free detection give an edge to Field Effect Transistor (FET) based biosensors among the other semiconductor-based biosensors. Presently, FET biosensors are principally used in various industries such as food and beverage, medicines, agriculture and environmental monitoring. The FET-based biosensors work on the principle of modulating the electrical parameters of the device with the dielectric constant of the biomolecules in the cavity. The existence or nonexistence of the target biomolecule in the cavity modifies the dielectric constant of the dielectric where the cavity has been created, which changes the drain current of the device [1–3]. Though the dielectrically modulated tunnel-FET (TFET) based sensor has gathered the focus of researchers, as it reduces short-channel effect, TFET-based sensors

suffer from high thermal budget requirements for source–drain formation and random dopant fluctuation arising from the difficulty in achieving the abrupt doping profile at source/drain–channel junctions [4]. Alternatively, Schottky barrier (SB) MOSFETs are considered as a prospective contender for high-performance CMOS ICs, as it is easy to form low-resistivity ultra-shallow junctions using metal source/drain instead of doped source/drain. Use of metal source/drain contact holds the advantage, as it commendably minimizes the issue of higher S/D series resistance and lessens the severe limitations imposed on conventionally implanted S/D. Further, intrinsic Schottky potential barrier of SB-MOSFETs results in greater control of OFF-state leakage current, and the subthreshold slope (SS) of SB-MOSFET has a lower limit of 60 mV/dec at room temperature [5–10]. Features such as low thermal budget requirements, higher invulnerability to short-channel effects, low source/drain (S/D) parasitic resistances, sub-10 nm gate length scalability and simple fabrication steps make Schottky barrier MOSFETs (SB-MOSFETs) a suitable FET biosensor for the detection of different biomolecules [3,4]. Nevertheless, SB-MOSFETs have many advantages compared to conventional MOSFETs. The intrinsic Schottky barrier between metal S/D and the semiconductor results in lower drive current [11–13]. Many SB devices, like dual metal gate, source/drain pocket doping, work function engineering, and plasma-based structures have been suggested in recent years to resolve the difficulties of SB-MOSFET, including ambipolar conduction and lower drive current [14–20]. Sumit Kale et al. employed dual-material S/D SB MOS with erbium silicide as the main S/D material and hafnium metal as the S/D extension material to suppress ambipolar leakage current in the SB-MOSFET [14]. Highly doped, dopant-segregated (DS) layers, which modulate the Schottky barrier (SB) height and width for improving the drive current of conventional SB-MOSFET, have been explored [15,16]. However, DS SB-MOSFET suffers from random dopant fluctuations (RDF) and increased thermal budget. Source engineered (SE) SB-MOSFET, using the charge-plasma concept to modify the SB width to eliminate RDF, has been studied. However, SE SBMOS suffer from ambipolar leakage current even for negative gate bias [17,18]. X Liu et al. have proposed the novel high-SB, bidirectional tunnel field effect transistor, which results in reduced thermionic emission and robust band-to-band (BTBT) forward tunneling current [10]. Sangeeta Singh et al. investigated the charge-plasma SB tunnel FET (CP-SB-TFET), and this study reveals that a pocket at both the drain and source end results in reduced ambipolar current, DIBL, and improved drive current [19]. Sumit Kale et al. have demonstrated that dopant segregation (DS) at the source-channel junction aids to increase tunneling area, which results in improved device performance with high ON current [20]. A ferroelectric SB tunnel FET (Fe SB-TFET) with a highly doped pocket at the source/drain and channel interface and gate–drain underlap reduce tunneling barrier width at the source side SB, resulting in improved device performance with low subthreshold swing (SS), reduced ambipolar current and high I_{ON}/I_{OFF} [6]. Investigation of temperature's effect on reliability issues of ferroelectric DS SB TFET reveals that the presence of a ferroelectric layer and the resulting negative capacitance effect increases the ON current, achieves highest I_{ON}/I_{OFF} ratio and reduces the SS to 23 mV/dec at 300 K [21]. Silicon on insulator SB-MOSFET (SOI SB-MOSFET) with source extension (SE) and with source drain extension (SDE) significantly reduces drain-induced barrier tunneling and produces higher I_{ON}/I_{OFF} and lower subthreshold swing (SS) than SOI SB-MOSFET [22].

The motivation of this work is to improve the performance of SB-MOSFET using structural modification and with source engineering. With this objective, a novel SB-MOSFET was made with quad gate structure and with SiGe at the source side of the channel. In this work, novel SB-MOSFET, named as quad gate SB-MOSFET, has been designed using TCAD, and its performance is analyzed using different electrical parameters such as ON current, I_{ON}/I_{OFF} and subthreshold slope (SS). With this novel quad gate structure and source engineering, both I_{ON}/I_{OFF} ratio and subthreshold slope have been improved. To substantiate, the performance improvement of the proposed quad gate SB-MOSFET's electrical parameters is compared to the double gate SB-MOSFET. In this work, double

gate SB-MOSFET is referred to as the conventional device as it has already been reported in the literature [23,24]. Further, the proposed device is used as a biosensor for detecting different biomolecules such as DNA, cellulose, APTES, biotin and streptavidin. This paper is organized as follows. The device structure and simulation approach are given in Section II, and simulation results of the proposed device and its comparison to the conventional device are presented in Section III. Application of the proposed device as a biosensor is given in Section IV, and the conclusion and future work are given in Section V.

2. Device Structure and Simulation Strategy

A 2D schematic cross section of the novel SB-MOSFET and conventional double gate SB-MOSFET are shown in Figures 1 and 2, respectively. In both the devices, source is a heavily doped p-region with doping concentration of 10^{20} cm^{-3} and drain is n^+ doped with a concentration of 10^{18} cm^{-3} . The channel is p-type silicon with doping concentration of 10^{15} cm^{-3} . Lower doping in the channel region is preferred, as it improves the carrier mobility, resulting in higher drain current. With the objective of designing a novel structure, two gate electrodes, with one gate dielectric at the source side and another at the drain side of the channel, have been used in this work. Both HfO_2 and SiO_2 are used as the gate dielectrics. The gate electrode, along with a high- κ dielectric (HfO_2) at the source side of the channel, produces a higher electric field and enhances the tunneling rate, resulting in a higher ON-state current. Use of high- κ gate dielectric at the source side increases the internal electric field, and the high dielectric constant of HfO_2 increases gate capacitance, resulting in a higher $I_{\text{ON}}/I_{\text{OFF}}$ ratio of the proposed device. Further, high- κ dielectric reduces the OFF-state leakage current due to direct tunneling, as it enables the use of a thicker gate oxide for the same gate capacitance, thereby reducing the power dissipation. The gate electrode at the drain side, along with SiO_2 as gate dielectric, broadens the barrier at the drain/channel junction and prevents carrier tunneling, thereby suppressing the ambipolar current [24,25]. Aluminum with a work function of 4.1 eV is used as the metal contact. Aluminum at the source and drain, along with silicon substrate, form a Schottky contact. In the proposed device, the gate is not continuous throughout the channel and is present only at the source and drain side of the channel. The gate at the source side improves the tunneling, while the gate at the drain side reduces the leakage current. As there are four gate contacts, two at the top side and two at the bottom side of the channel, the name “quad gate” was given to the proposed SB-MOSFET. In this work, the gate structure is novel, i.e., the gate is present only at the source side and drain side of the channel. Further, to improve the carrier mobility, SiGe is introduced at the source side of the channel. Use of SiGe at the source side, and the resulting lower Schottky barrier, enhance the injection of the electron into the channel, thereby improving current drive capability. In contrast, a higher Schottky barrier for holes effectively suppresses hole injection into the silicon channel, thereby preventing the flow of holes in the OFF-state. Further, SiGe improves electron mobility by straining the crystal lattice, resulting in higher drive currents [26,27]. Silvaco TCAD is used for the design and simulation of the proposed device. The Universal Schottky Tunneling (UST) model captures tunneling close to the source channel junction while mobility models, viz., concentration mobility (CONMOB) and field dependent mobility (FLDMOB), have been used to capture different types of mobility. Band-gap narrowing models take into account the band-gap narrowing due to high doping concentrations of the source and drain while the Shockley–Read–Hall (SRH) model captures the effect of thermal generation leakage currents. Further, the transport mechanism in the device is simulated by the drift-diffusion model. Table 1 shows the parameters of different regions of both the proposed and conventional devices considered for simulation.

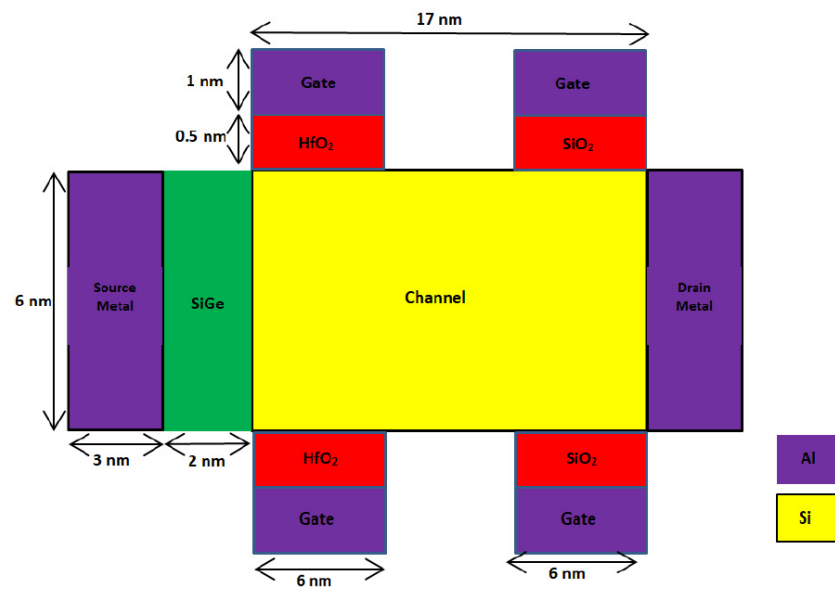


Figure 1. Schematic cross section of proposed quad gate SB-MOSFET.

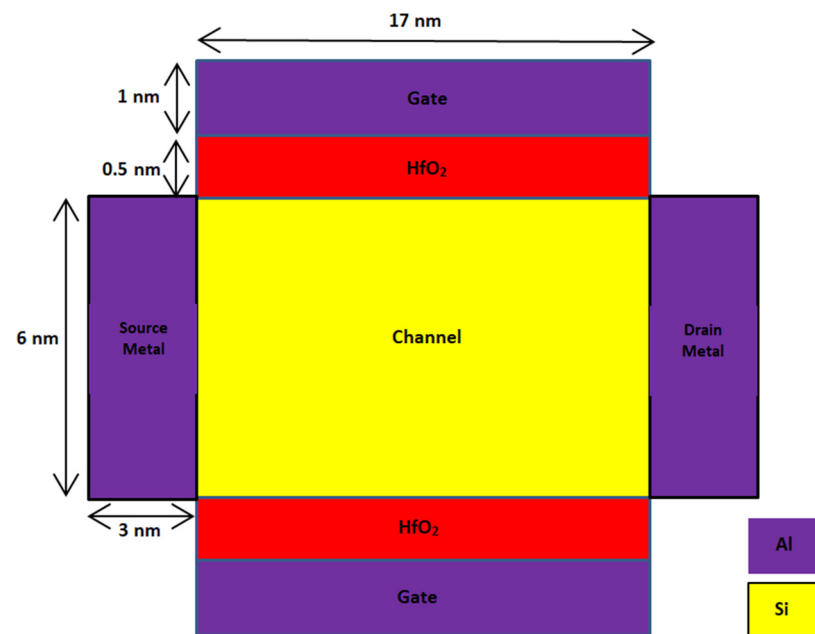


Figure 2. Schematic cross section of conventional double gate SB-MOSFET.

Table 1. Simulation parameter of proposed quad gate and conventional DG SB-MOSFET.

Parameter	Quad Gate SB-MOSFET	Conventional SB-MOSFET
Gate oxide thickness	0.5 nm	0.5 nm
Silicon thickness	6 nm	6 nm
Source length	2 nm	2 nm
Doping concentration of Source	1020 cm^{-3}	1020 cm^{-3}
Doping concentration of drain	1018 cm^{-3}	1018 cm^{-3}
Channel length	17 nm	17 nm
Doping concentration of channel	1015 cm^{-3}	1015 cm^{-3}
Thickness of SiGe	6 nm	-
Length of SiGe	2 nm	-

3. Result and Discussion

Different electrical characteristics, viz., surface potential, electric field, band energy and transfer characteristics of both the proposed and conventional DG SB-MOSFET, are analyzed and the corresponding results are presented in Figures 3–6. It should be noted that in Figures 3–5, the left end of the plot represents the drain side, while the right end corresponds to the source side of the channel. Surface potential variation along the channel length of both the proposed and conventional SB-MOSFET is presented in Figure 3. It has been observed that surface potential, a vital factor in estimating the DC property of thin-film transistor, is better in the proposed quad gate SB-MOSFET than in the conventional SB-MOSFET. The surface potential is almost 50% higher for the proposed device than conventional device. The surface potential is 1.15 V for the proposed device while the value is 0.75 V for the conventional device at $0.0215 \mu\text{m}$ for the bias voltage of $V_{gs} = 0.5 \text{ V}$ and $V_{ds} = 0.8 \text{ V}$. Figure 4 presents variation of the electric field across the channel of both devices. It has been observed that the proposed quad gate SB-MOSFET produces a higher electric field at both the source and drain side of the channel than the conventional SB-MOSFET. The electric field is approximately three times higher in the quad gate SB-MOSFET than the conventional device. The electric field is 5.7 MV/cm in the proposed device while the value is 1.9 MV/cm in the conventional device. This higher electric field results in higher tunneling current, as BTBT generation rate is a strong function of the electric field. It can also be observed that in the proposed device, the electric field at the source/channel junction is higher than that value at the drain/channel junction. This could be attributed to the effect of the different gate electrodes at the source and drain side of the channel. HfO_2 at the source side of the channel produces a higher electric field, which is useful for achieving a higher tunneling rate. The lower electric field resulting from the use of SiO_2 as a gate dielectric at the drain side of the channel is useful for inhibiting tunneling of charges in the ambipolar state.

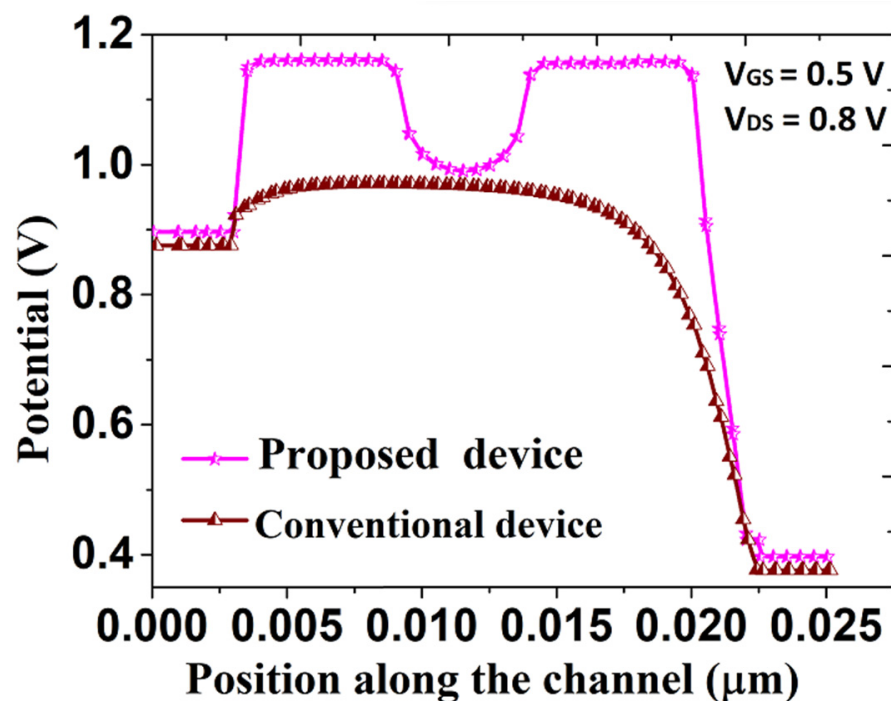


Figure 3. Variation of surface potential of proposed and conventional SB-MOSFET.

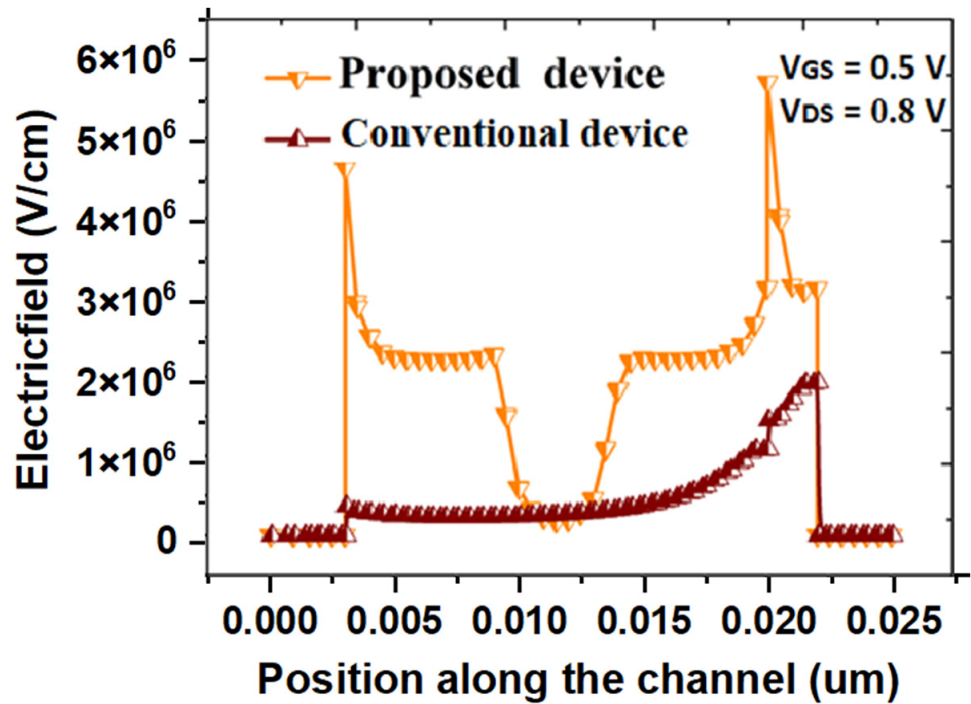


Figure 4. Variation of electric field of proposed and conventional SB-MOSFET.

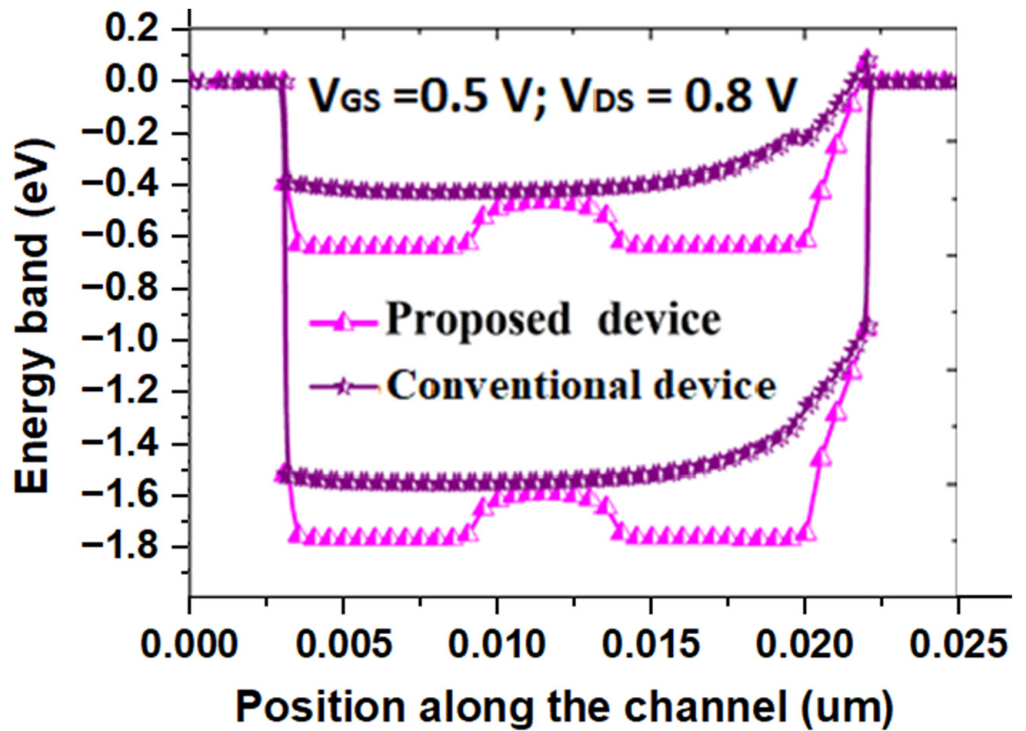


Figure 5. Energy band diagram of proposed and conventional SB-MOSFET.

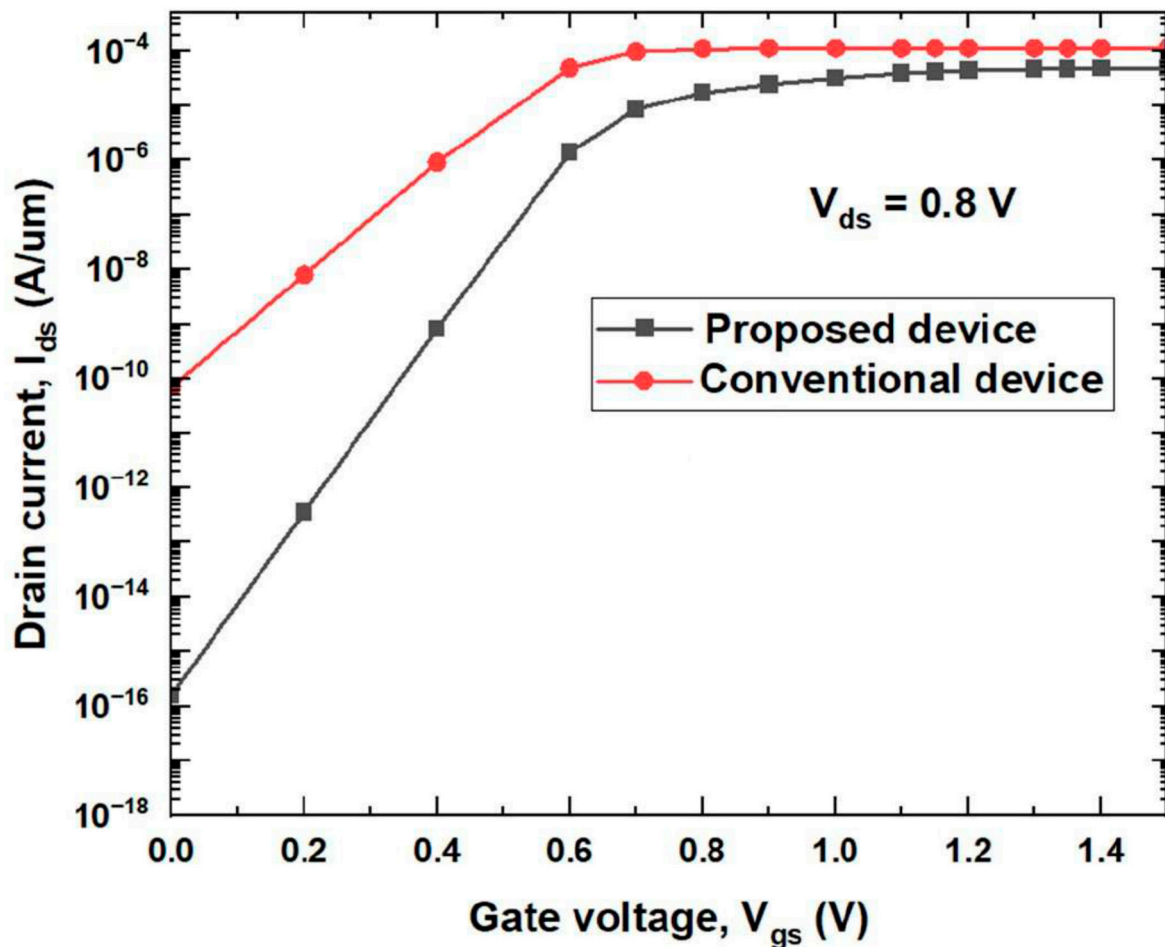


Figure 6. Comparison of transfer characteristics of proposed device with conventional device.

Figure 5 shows variation of the energy band along the channel length of both the SB-MOSFETs. The energy band diagram is measured at the gate–source voltage (V_{GS}) of 0.5 V and drain–source voltage (V_{DS}) of 0.8 V. It could be observed that the energy barrier width is significantly reduced at source side of the channel at the position of $0.0225 \mu\text{m}$ for the proposed quad gate SB-MOSFET than for the conventional device. The reason for SB thinning at the source side of the channel could be attributed to the use of a high- κ gate dielectric combined with the SiGe pocket region at the source side of the channel. A thinner energy barrier results in higher tunneling of electrons through the channel. Figure 6 presents drain current versus gate voltage characteristics of the proposed quad gate SB-MOSFETs compared to the conventional DG SB-MOSFET. It has been observed that there is a slight decrease in the ON current of quad gate SB-MOSFET; however, the proposed device exhibits a much lower OFF-state current. The OFF-state current of the proposed device is more than five orders lower than the conventional device. A significantly lower OFF-state current in the proposed device could be attributed to two reasons. The presence of the SiGe pocket region at the source side of the channel acts as an additional barrier in the OFF-state, ensuing in low leakage current. The other reason is aluminum, along with SiO_2 at the drain side of the channel, broadens the drain/channel junction barrier, which results in a low tunneling probability of hole through the drain-side SB. It can also be observed that in the subthreshold region, there is a sharp decrease in drain current with respect to gate voltage in the proposed device compared to the conventional one, resulting in better subthreshold behavior of the proposed device. Electrical parameters of both the proposed and conventional DG SB-MOSFETs, calculated from the transfer characteristics, are compared and the results are given in Table 2. The proposed device exhibits superior

performance with improved I_{ON}/I_{OFF} ratio and reduced SS. The I_{ON}/I_{OFF} ratio of the quad gate SB-MOSFET is five orders more than the conventional device while the subthreshold slope of quad SB-MOSFET is 25% lower than that of the conventional device. These results imply that the quad gate SB-MOSFET is suitable for future nano-scale ICs.

Table 2. Comparison of electrical parameters of proposed and conventional SB-MOSFET.

Parameter	Quad Gate SB-MOSFET	Conventional SB-MOSFET
I_{ON}	0.5×10^{-4}	10^{-4}
I_{OFF}	1.5×10^{-16}	9×10^{-11}
I_{ON}/I_{OFF}	3.3×10^{11}	1.1×10^6
SS (mV/dec)	60.65	75.81

4. Applications

Biosensors have had a long journey, beginning from ion-sensitive FET [28] with a high sensitivity only to charged biomolecules like DNA, to present-day biosensors, which can detect neutral biomolecules like biotin and streptavidin. Biomolecules exist in different forms extending from nucleic acid, viruses, bacteria and proteins, and dimensions ranging from nm to μm . Knowledge of how these biomolecules function and their impact on several fields such as medicine, agriculture, and the food industry necessitated the early detection of biomolecules [29–34]. FET-based biosensors are realized by carving out a nanocavity at the source and/or drain end of the MOSFET. Existence of biomolecules in the nanocavity results in a change in the coupling between the gate and channel due to a change in dielectric constant of the gate oxide [34]. Further, this change in the dielectric constant results in SB thinning, resulting in higher tunneling current. Change in the drain current of the proposed quad gate SB-MOSFET biosensor can be used as an electrical parameter to detect the target biomolecules. The ability of the biosensor to detect the target biomolecules can be determined using the parameter of drain current sensitivity (S_{ID}) and is given by [7]

$$S_{I_{ON}} = \frac{I_{Bio} - I_0}{I_0} \quad (1)$$

where I_{Bio} and I_0 represent the ON-state current in the presence and absence of the biomolecules in the nanocavity, respectively. Higher sensitivity implies a higher chance of detecting the target species. Few works on FET-based biosensors have been reported in the literature [1,7]. S.A. Hafiz et al. have proposed source-engineered SB-FET, using the charge-plasma concept for sensing biomolecules, and observed that SE SB-FET exhibit much higher sensing capability for both neutral and charged biomolecules [1]. The L-shaped SB-FET biosensor designed with Al and Cu as a dual-material gate and with HfO_2 as a gate dielectric exhibit better sensitivity at both low and high temperatures [7]. In this work, the proposed quad gate SB-MOSFET can be used as a biosensor for label-free detection of both charged and neutral biomolecules. The proposed device is converted into a biosensor by creating a nanocavity by etching gate oxide (HfO_2) near the source junction of the channel. The size of the nanocavity is $4 \text{ nm} \times 0.5 \text{ nm}$. The proposed biosensor can be used for detecting different biomolecules such as streptavidin, biotin, APTES, cellulose and DNA which have unique dielectric constants, as given in Table 3. Biomolecules are placed in the nanocavity near the source end of the channel, and the corresponding variation in different electrical parameters such as surface potential, electric field and drain current are observed. The presence of different biomolecules in the nanocavity is modeled as oxide having different dielectric constants, as shown in Figure 7. To mirror the influence of a charged biomolecule, a fixed-interface oxide charge is included in the dielectric layer.

Figure 8 shows the electric field variation across the channel with different biomolecules in the nanocavity. It can be seen that the electric field near the source end of the channel is highest for DNA and lowest for streptavidin, which concludes that the electric field

increases with dielectric constant of the biomolecules. This could be attributed to the decrease in width of the depletion region due to thinning of the Schottky barrier, resulting in a higher electric field near the source.

Table 3. Dielectric constant of biomolecules.

S.No	Biomolecules	Dielectric Constant
1	Streptavidin	2.1
2	Biotin	2.63
3	APTES	3.57
4	Cellulose	6.1
5	DNA </td <td>8.7</td>	8.7

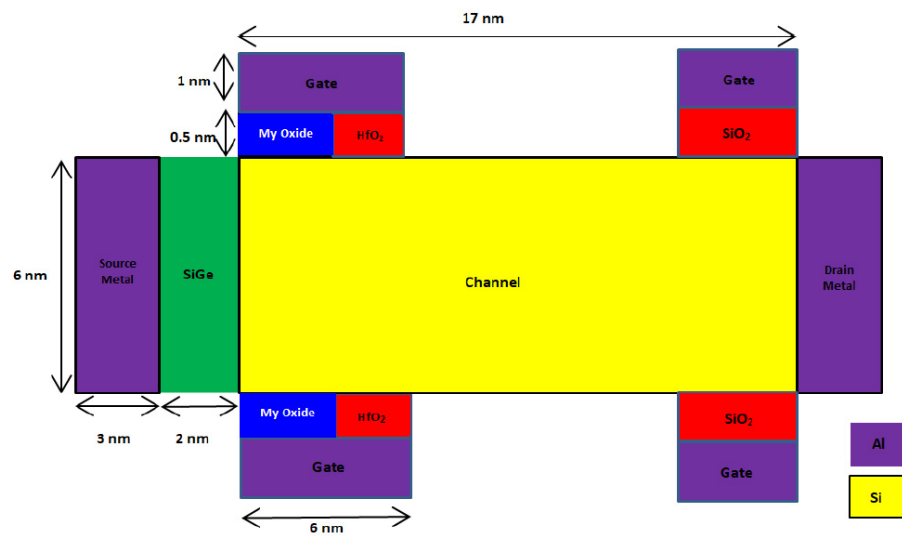


Figure 7. Schematic cross section of proposed quad gate SB-MOSFET Biosensor.

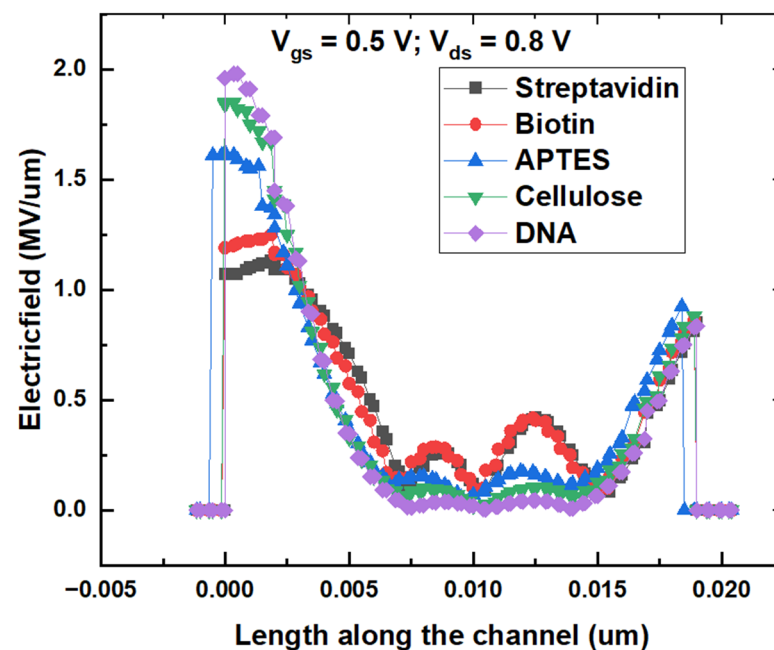


Figure 8. Electric field variation of proposed biosensor with different biomolecules.

Figure 9 shows the surface potential variation across the channel length with different biomolecules. It could be observed that potential is higher for biomolecules that have a higher dielectric constant, which could be ascribed to an increase in the capacitance with the dielectric constant of biomolecules in the cavity.

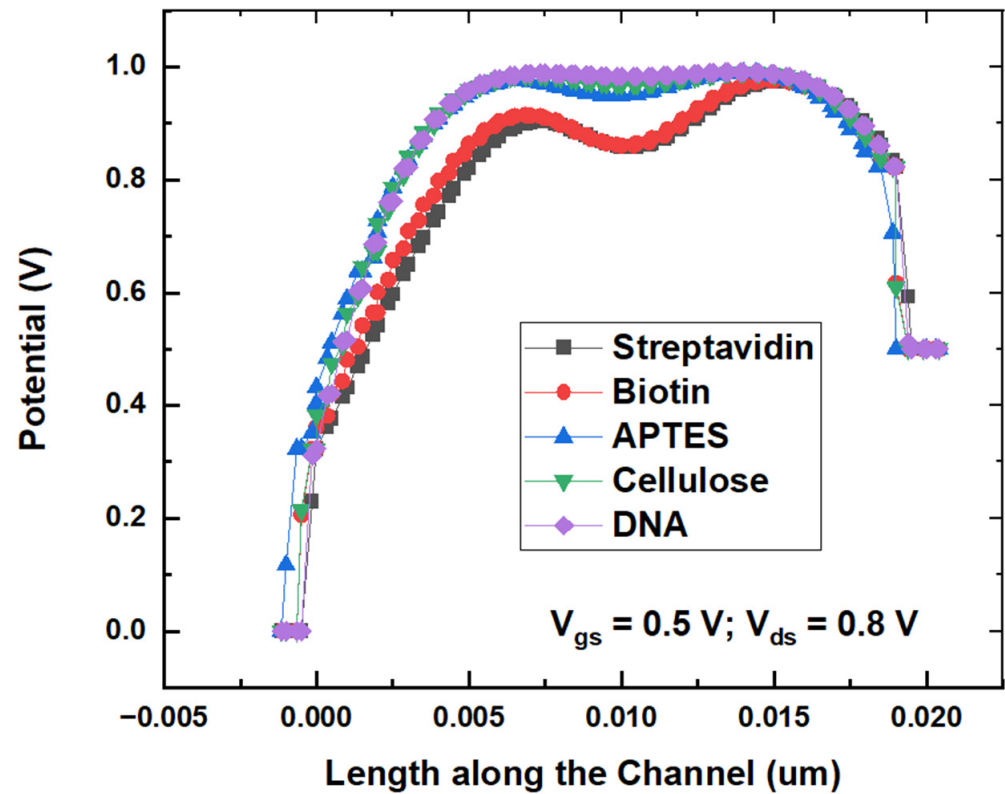


Figure 9. Surface potential variation for the proposed biosensor with different biomolecules.

It could be observed from Figure 10 that, for lower gate voltage, drain current increases with the dielectric constant, as DNA exhibits higher drain current while streptavidin produces lower drain current. An increase in the coupling capacitance with the dielectric constant results in higher charge concentration in the channel, resulting in an increase in drain current with the dielectric constant of the biomolecules. Surface potential variation along the length of the channel and transfer characteristics given in Figures 9 and 10 are almost matching for both the biomolecules streptavidin and biotin. A small difference between the dielectric constants could be the reason behind almost-identical responses to these two biomolecules. To demonstrate the advantage of the proposed biosensor for the detection of different biomolecules, conventional biosensors are also designed by creating a nanocavity near the source side of the channel in the dielectric. Both the cross section and transfer characteristics of conventional biosensors are given in Figures 11 and 12, respectively.

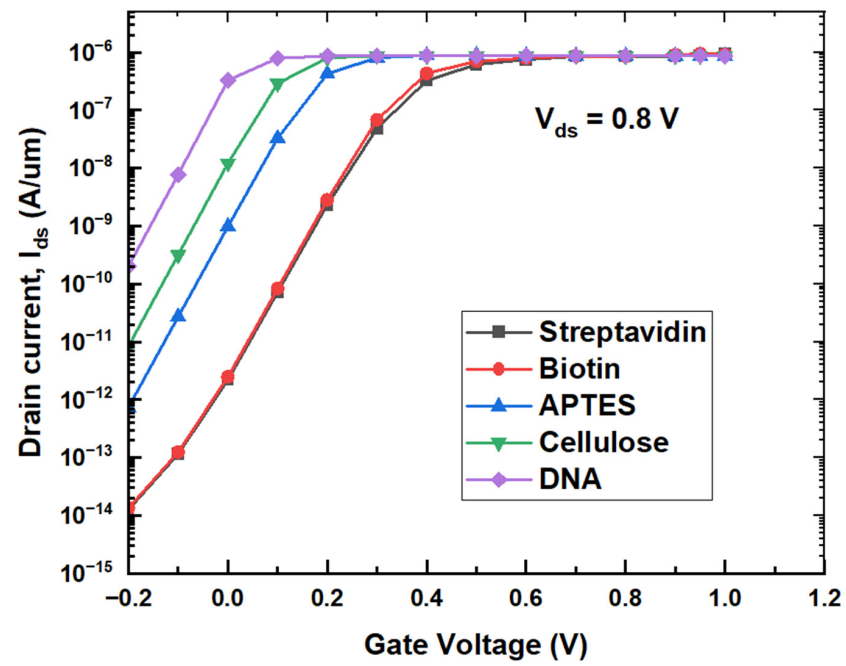


Figure 10. Transfer characteristics of proposed biosensor with different biomolecules.

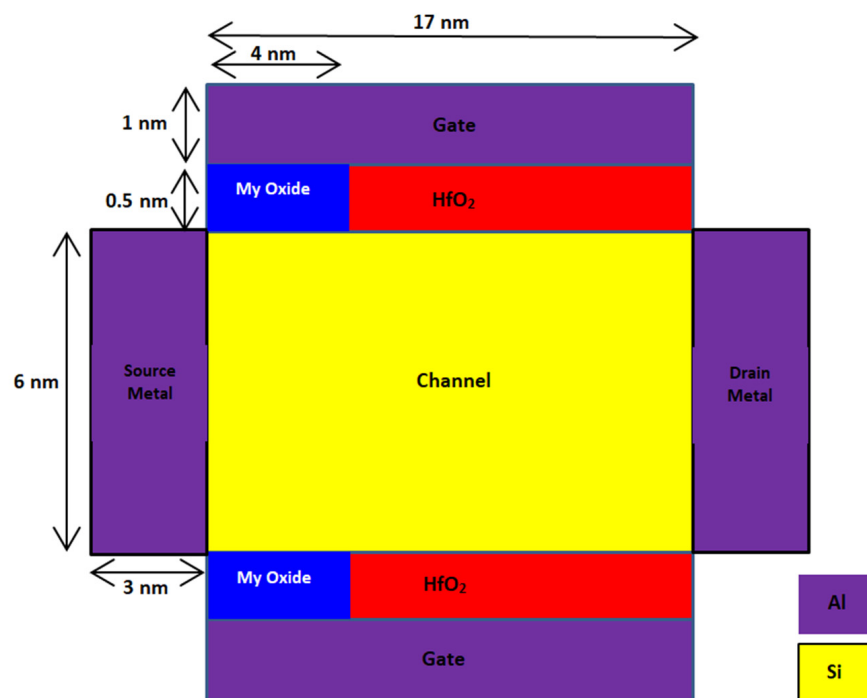


Figure 11. Schematic cross section of conventional DG SB-MOSFET Biosensor.

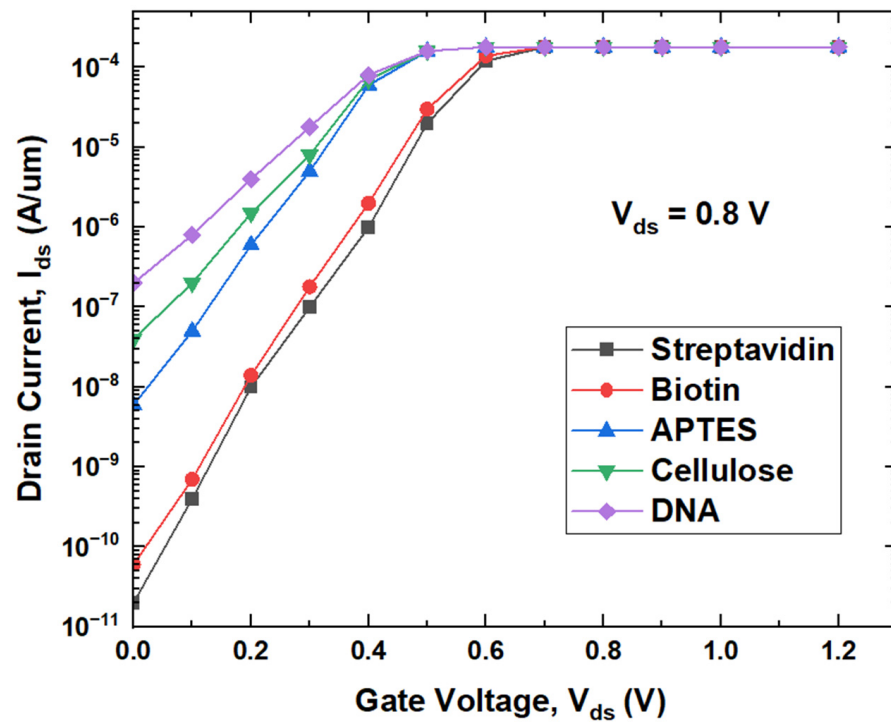


Figure 12. Transfer characteristics of conventional biosensor with different biomolecules.

Drain current sensitivity (S_{ID}) of both the conventional and proposed biosensors are calculated by using the Equation (1) at the gate to source voltage of 0.5 V and given in Figure 13.

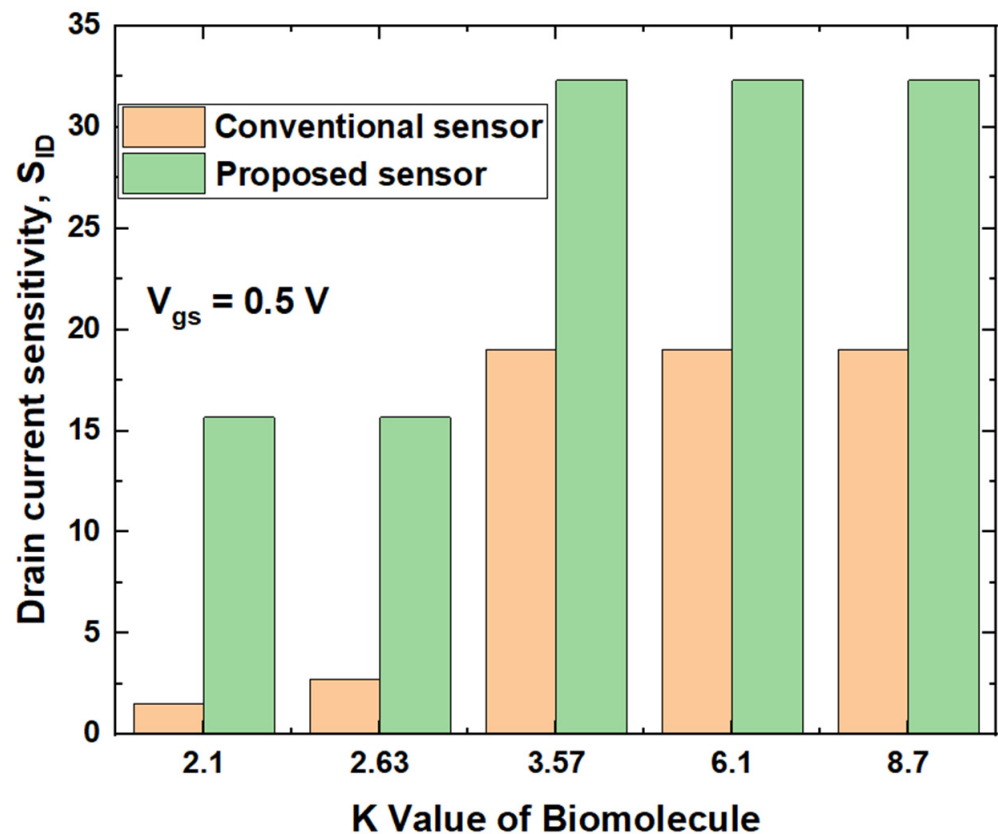


Figure 13. Comparison of drain current sensitivity of proposed and conventional biosensors.

It can be observed that drain current sensitivity (S_{ID}) increases with the increase in the dielectric constant, and the change is better in the proposed device than the conventional sensor made from DG SB-MOSFET. This could be ascribed to enhanced SB thinning resulting in a higher ON-current of the proposed device. Further, the S_{ID} value of biomolecules such as APTES, cellulose and DNA of the proposed sensor is found to be twice that of streptavidin and biotin. The S_{ID} value of DNA is 32.33 while the value of biotin is 15.67. This sensitivity analysis implies that the proposed biosensor outperforms the conventional sensor in the detection of all the five molecules and sensitivity is higher for biomolecules having a dielectric constant of more than 3.5. Selectivity is one of the vital parameters of the biosensor that determine how effectively the sensor detects the target biomolecule among the other biomolecules present in the cavity. Selectivity is calculated by taking the relative ratio of the drain current at different dielectric constant and is given by [31]

$$\Delta S = \frac{I_{ON}(k = 3.57, 6.1, 8.7) - I_{ON}(k = 2.63)}{I_{ON}(k = 2.63)} \quad (2)$$

Figure 14 presents the selectivity of biotin among the APTES, cellulose and DNA of both the proposed and conventional sensors. It could be observed that selectivity of the proposed sensor is six to twelve times higher than the conventional sensor based on the target biomolecules.

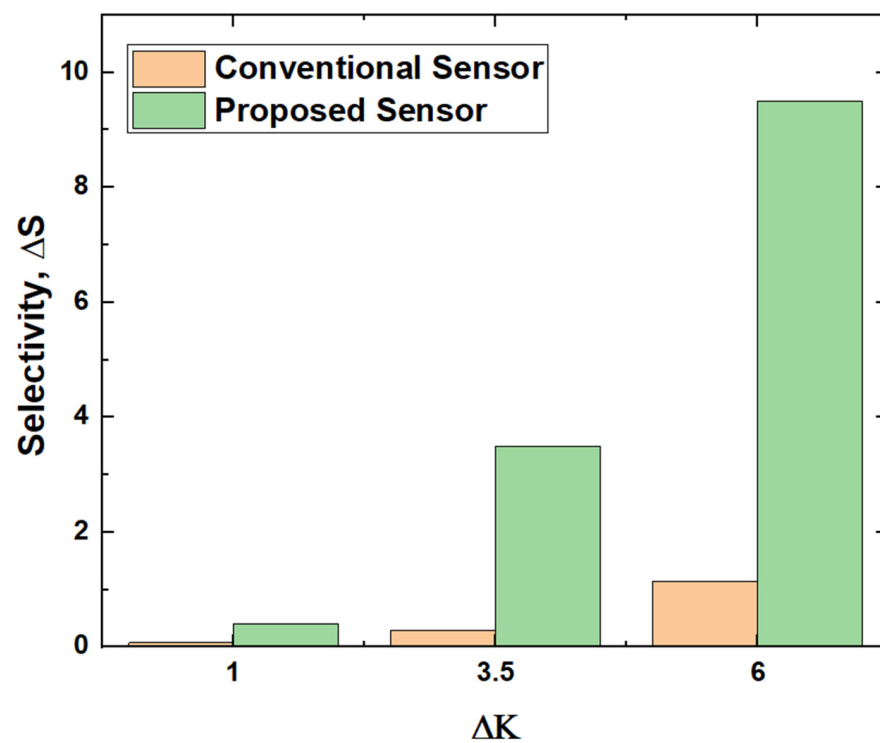


Figure 14. Selectivity of proposed and conventional biosensor.

5. Conclusions

In this paper, the novel SB-MOSFET-based biosensor for detecting the changes in physiological parameters of living organism has been proposed. The proposed device consists of a quad gate with a SiGe pocket region near the source end of the channel. Use of high- κ gate dielectric at the source end of the channel produces a higher electric field and enhances tunneling probability. On the other hand, SiO₂ as the gate dielectric at the drain end broadens SB at the drain/channel junction, resulting in a reduced OFF-state current. The proposed device is found to be suitable for nano biosensors for detecting various biomolecules as it exhibits better electrical characteristics with a higher I_{ON} - I_{OFF}

ratio and lower subthreshold slope. The I_{ON} - I_{OFF} ratio of the proposed device is six orders higher than the conventional double gate SB-MOSFET, and the subthreshold slope is 25% lower than that of the conventional device. Biosensors, both the proposed and conventional devices, are made by creating a nanocavity near the source end of the channel. It has been observed that drain current sensitivity increases with the dielectric constant of the biomolecules in the cavity. It is concluded that the proposed quad gate SB-MOSFET Biosensor has exceptional biosensing capability with higher sensitivity and selectivity than conventional bio sensors made from DG SB-MOSFET. In the future, further modification of the proposed device is required to distinguish biomolecules that have slightly different dielectric constants.

Author Contributions: Conceptualization, P.K.; Software, A.V.; Writing—original draft, P.E.; Writing—review & editing, M.E. All authors have read and agreed to the published version of the manuscript.

Funding: This research received no external funding.

Data Availability Statement: Not applicable.

Conflicts of Interest: The authors declare no conflict of interest.

References

- Hafiz, S.A.; Iltesha; Ehteshamuddin, M.; Loan, S.A. Dielectrically Modulated Source-Engineered Charge-Plasma-Based Schottky-FET as a Label-Free Biosensor. *IEEE Trans. Electron Devices* **2019**, *66*, 1905–1910. [\[CrossRef\]](#)
- Rashid, S.; Bashir, F.; Khanday, F.A.; Beigh, M.R. Double Gate 6H-Silicon Carbide Schottky Barrier FET as Dielectrically Modulated Label Free Biosensor. *Silicon* **2022**, 1–12. [\[CrossRef\]](#)
- Sen, D.; De, A.; Goswami, B.; Shee, S.; Sarkar, S.K. Noise Immune Dielectric Modulated Dual Trench Transparent Gate Engineered MOSFET as a Label Free Biosensor: Proposal and Investigation. *J. Comput. Electron.* **2021**, *20*, 2594–2603. [\[CrossRef\]](#) [\[PubMed\]](#)
- Ghosh, B.; Akram, M.W. Junctionless tunnel field effect transistor. *IEEE Electron Device Lett.* **2013**, *34*, 584–586. [\[CrossRef\]](#)
- Larson, J.M.; Snyder, J. Overview and status of metal S/D Schottky barrier MOSFET technology. *IEEE Trans. Electron Devices* **2006**, *53*, 1048–1058. [\[CrossRef\]](#)
- Kale, S.; Kondekar, P.N. Ferroelectric Schottky barrier tunnel FET with gate-drain underlap: Proposal and investigation. *Superlattices Microstruct.* **2016**, *89*, 225–230. [\[CrossRef\]](#)
- Rashid, S.; Bashir, F.; Khanday, F.A.; Beigh, M.R. L-Shaped High Performance Schottky Barrier FET as Dielectrically Modulated Label Free Biosensor. *IEEE Trans. NanoBiosci.* **2022**, *21*, 542–548. [\[CrossRef\]](#)
- Calvet, L.E.; Luebben, H.; Reed, M.A.; Wang, C.; Snyder, J.P. Subthreshold and scaling of PtSi Schottky barrier MOSFETs. *Superlattices Microstruct.* **2000**, *28*, 501–506. [\[CrossRef\]](#)
- Liu, X.; Ma, K.; Wang, Y.; Wu, M.; Lee, J.-H.; Jin, X. A Novel High Schottky Barrier Based Bilateral Gate and Assistant Gate Controlled Bidirectional Tunnel Field Effect Transistor. *IEEE J. Electron Devices Soc.* **2020**, *8*, 976–980. [\[CrossRef\]](#)
- Imenabadi, R.M.; Saremi, M.; Vandenberghe, W.G. A Novel PNP-Like Z-Shaped Tunnel Field-Effect Transistor With Improved Ambipolar Behavior and RF Performance. *IEEE Trans. Electron Devices* **2017**, *64*, 4752–4758. [\[CrossRef\]](#)
- Sharma, S.; Goel, A.; Rewari, S.; Nath, V.; Gupta, R.S. Gallium Nitride Cylindrical Schottky Barrier MOSFET(GaN-CSB-MOSFET) For High-Frequency Implementation. In Proceedings of the 2021 International Conference on Industrial Electronics Research and Applications (ICIARA), New Delhi, India, 22–24 December 2021; pp. 1–6. [\[CrossRef\]](#)
- Agarwal, L.; Priya, G.L.; Papnassam, E.; Kumar, B.P.; Venkatesh, M. A Novel Metal Dielectric Metal Based GAA-Junction-Less TFET Structure for Low Loss SRAM Design. *Silicon* **2022**, 1–13. [\[CrossRef\]](#)
- Anusuya, P.; Kumar, P.; Esakki, P.; Agarwal, L. Recent Study on Schottky Tunnel Field Effect Transistor for Biosensing Applications. *Silicon* **2022**, *14*, 10187–10198. [\[CrossRef\]](#)
- Kale, S.; Kondekar, P.N. Charge plasma based source/drain engineered Schottky Barrier MOSFET: Ambipolar suppression and improvement of the RF performance. *Superlattices Microstruct.* **2018**, *113*, 799–809. [\[CrossRef\]](#)
- Knoll, L.; Schfer, A.; Trellenkamp, S.; Bourdelle, K.K.; Zhao, Q.T.; Mantl, S. Nanowire and planar UTB SOI Schottky Barrier MOSFETs with dopant segregation. In Proceedings of the 13th International Conference on Ultimate Integration on Silicon (ULIS), Grenoble, France, 6–7 March 2012.
- Knoch, J.; Zhang, M.; Zhao, Q.T.; Mantl, S. Schottky-barrier height tuning using dopant segregation in Schottky-barrier MOSFETs on fully-depleted SOI. *MRS Online Proc. Libr. (OPL)* **2006**, *913*, 0913-D01. [\[CrossRef\]](#)
- Kale, S.; Kondekar, P.N. Design and Investigation of Dielectric Engineered Dopant Segregated Schottky Barrier MOSFET With NiSi Source/Drain. *IEEE Trans. Electron Devices* **2017**, *64*, 4400–4407. [\[CrossRef\]](#)
- Kale, S. Investigation of Dual Metal Gate Schottky Barrier MOSFET for Suppression of Ambipolar Current. *IETE J. Res.* **2023**, *69*, 404–409. [\[CrossRef\]](#)

19. Singh, S.; Singh, A.P.; Kondekar, P.N. A novel self-aligned charge plasma Schottky barrier tunnel FET using work function engineering. *Microelectron. Eng.* **2017**, *168*, 67–75. [[CrossRef](#)]
20. Kale, S.; Chandu, M.S. Dual Metal Gate Dielectric Engineered Dopant Segregated Schottky Barrier MOSFET With Reduction in Ambipolar Current. *Silicon* **2022**, *14*, 935–941. [[CrossRef](#)]
21. Ghosh, P.; Bhowmick, B. Effect of Temperature on Reliability Issues of Ferroelectric Dopant Segregated Schottky Barrier Tunnel Field Effect Transistor (Fe DS-SBTFT). *Silicon* **2020**, *12*, 1137–1144. [[CrossRef](#)]
22. Kumar, P.; Bhowmick, B. Source-Drain Junction Engineering Schottky Barrier MOSFETs and their Mixed Mode Application. *Silicon* **2020**, *12*, 821–830. [[CrossRef](#)]
23. Mukhopadhyay, A.; Bhattacharya, S.; Gupta, P.S.; Banerjee, L.; Sengupta, A.; Rahaman, H. A Hybrid Atomistic—Semi-Analytical Modeling on Schottky Barrier Au-MoS₂-Au MOSFETs. In Proceedings of the 2018 IEEE Electron Devices Kolkata Conference (EDKCON), Kolkata, India, 24–25 November 2018; pp. 46–50. [[CrossRef](#)]
24. Rashid, S.; Bashir, F.; Khanday, F.A.; Beigh, M.R.; Hussin, F.A. 2-D Design of Double Gate Schottky Tunnel MOSFET for High-Performance Use in Analog/RF Applications. *IEEE Access* **2021**, *9*, 80158–80169. [[CrossRef](#)]
25. Soni, D.; Sharma, D.; Yadav, S.; Aslam, M.; Yadav, D.S.; Sharma, N. Gate Metal Work Function Engineering for the Improvement of Electrostatic Behaviour of Doped Tunnel Field Effect Transistor. In Proceedings of the 2017 IEEE International Symposium on Nano-electronic and Information Systems (iNIS), Bhopal, India, 18–20 December 2017; pp. 190–194. [[CrossRef](#)]
26. Vinod, A.; Kumar, P.; Bhowmick, B. Impact of ferroelectric on the electrical characteristics of silicon–germanium based heterojunction Schottky barrier FET. *AEU Int. J. Electron. Commun.* **2019**, *107*, 257–263. [[CrossRef](#)]
27. Ikeda, K.; Yamashita, Y.; Endoh, A.; Fukano, T.; Hikosaka, K.; Mimura, T. 50-nm gate Schottky source/drain p-MOSFETs with a SiGe channel. *IEEE Electron Device Lett.* **2002**, *23*, 670–672. [[CrossRef](#)]
28. Bergveld, P. Development, operation, and application of the ionsensitive field-effect transistor as a tool for electrophysiology. *IEEE Trans. Biomed. Eng.* -19.
29. Dwivedi, P.; Singh, R.; Sengar, B.S.; Kumar, A.; Garg, V. A New Simulation Approach of Transient Response to Enhance the Selectivity and Sensitivity in Tunneling Field Effect Transistor-Based Biosensor. *IEEE Sens. J.* **2020**, *21*, 3201–3209. [[CrossRef](#)]
30. Kumar, A.; Roy, M.; Gupta, N.; Tripathi, M.M.; Chaujar, R. Dielectric modulated transparent gate thin film transistor for biosensing applications. *Mater. Today Proc.* **2020**, *28*, 141–145. [[CrossRef](#)]
31. Liu, H.; Lei, Y. A critical review: Recent advances in “digital” biomolecule detection with single copy sensitivity. *Biosens. Bioelectron.* **2021**, *177*, 112901. [[CrossRef](#)]
32. Barman, U.; Goswami, N.; Ghosh, S.S.; Paily, R.P. Fabrication of FET Biosensor for Detection of Glutathione. In Proceedings of the 2018 4th IEEE International Conference on Emerging Electronics (ICEE), Bengaluru, India, 17–19 December 2018; pp. 1–4.
33. Dewan, B.; Chaudhary, S.; Yadav, M. Evaluating the Performance Parameters of Triple Metal Dual Gate Vertical Tunnel FET Biosensor. In Proceedings of the 2022 IEEE International Students’ Conference on Electrical, Electronics and Computer Science (SCEECS), Bhopal, India, 19–20 February 2022; pp. 1–5.
34. Im, H.; Huang, X.-J.; Gu, B.; Choi, Y.-K. A dielectric-modulated field-effect transistor for biosensing. *Nat. Nanotechnol.* **2007**, *2*, 430–434. [[CrossRef](#)] [[PubMed](#)]

Disclaimer/Publisher’s Note: The statements, opinions and data contained in all publications are solely those of the individual author(s) and contributor(s) and not of MDPI and/or the editor(s). MDPI and/or the editor(s) disclaim responsibility for any injury to people or property resulting from any ideas, methods, instructions or products referred to in the content.